International Journal of Power Electronics and Drive Systems (IJPEDS)
Vol. 14, No. 3, September 2023, pp. 1374~1381
ISSN: 2088-8694, DOI: 10.11591/ijpeds.v14.i3.pp 1374-1381

Field oriented controlled permanent magnet synchronous motor drive for an electric vehicle

Chau Si Thien Dong[1], Hoang Huy Le[2], Hau Huu Vo[1]
[1]Modeling Evolutionary Algorithms Simulation and Artificial Intelligence, Faculty of Electrical and Electronics Engineering, Ton Duc Thang University, Ho Chi Minh City, Vietnam
[2]Faculty of Electrical and Electronics Engineering, Ton Duc Thang University, Ho Chi Minh City, Vietnam

Article Info

Article history:

Received Nov 15, 2022
Revised Jan 10, 2023
Accepted Feb 6, 2023

Keywords:

Electric vehicle
Field oriented control
Performance indices
Permanent magnet synchronous motor
Space vector pulse width modulation

ABSTRACT

The paper describes field-oriented control strategy with space vector pulse width modulation technique of permanent magnet synchronous motor drive system for an electric vehicle. At first, mathematical models of the motor and the drive system for electric vehicle are presented. In order to obtain high performance drive and maximum motor torque, field-oriented control strategy and space vector pulse width modulation technique method are applied to drive system in next section. Speed controller design utilizing the popular zero-pole elimination approach causes large integral constant time in case of small rotational damping constant. The desired-transient-response-based approach is employed to overcome the problem. Performance indices include overshoot, undershoot, steady-state speed error, and total harmonic distortion of stator current, are employed to assess the drive systems with two speed controller design methods. Theoretical assumptions are confirmed via simulations and criteria in MATLAB/Simulink environment.

Corresponding Author:

Hau Huu Vo
Modeling Evolutionary Algorithms Simulation and Artificial Intelligence
Faculty of Electrical and Electronics Engineering, Ton Duc Thang University
19 Nguyen Huu Tho Street, Tan Phong Ward, District 7, Ho Chi Minh City, Vietnam
Email: vohuuhau@tdtu.edu.vn

1. INTRODUCTION

Electric vehicless (EVs) have been playing an important role in achieving allowable carbon levels [1], [2]. Among types of motor, permanent magnet synchronous motors (PMSMs) own suitable characteristics for EVs such as high start-up torque, small torque ripple, built-in magnetic field. For high-performance PMSM drives, direct torque control (DTC) [3]–[5] and field oriented control (FOC) [6]–[10] were utilized. A frame-angle-based DTC for PMSM drives was implemented to get fast and accurate responses at low speeds [3]. An improved DTC with large duty-cycle at transient operation was utilized to achieve fast response [4]. In order to obtain robust transient response, a duty-ratio regulation-based PMSM DTC was employed [5]. The FOC applied to PMSMs provided performance as well as DC motors [6]. The performance of FOC was discussed in drives utilizing hysteresis controller and pulse width modulation (PWM) current controller [7]. Maximum torque was enhanced by injecting current harmonic in FOC drive [8]. A space vector pulse width modulation (SVPWM) technique minimized switching loss in sensorless FOC drive [9]. In order to shorten computing time, a vector space decomposition approach was used in different FOC versions [10]. The FOC was utilized in sensorless drive at high speed [11]. In the paper, the FOC is selected for PMSM drive system of a modeled EV.

In order to ensure constant switching frequency of voltage source inverter (VSI), PWM techniques were utilized [12]–[21]. The SVPWM was implemented into sensorless drives [12]. Total harmonic distortions

(THDs), torque and speed responses, DC link utilization (DCLU) were evaluated for Sinusoidal PWM (SPWM) and SVPWM methods [13]. A PWM technique guaranteed on-time of the low-side switches and decreased capacitor current [14]. The SVPWM replaced for switching sequence selection method to lower torque ripple [15]. An added advantage of SVPWM compared to SPWM was an increase of DCLU [16]. Voltage error was calculated to make switching frequency almost constant [17]. The SVPWM was combined with Kalman filter to lower ripples [18]. A harmonic injecting method increased DCLU [19]. A PWM method lowered loss and current THD [20]. A modulation method shortened time harmonics [21]. For guarantee of constant switching frequency, and better DCLU, the SVPWM is utilized to control the VSI in the paper.

For controllers design of FOC drive, many approaches were presented [22]-[34]. Sliding mode theory and sigmoid function provided robustness of speed controller and chattering elimination [22]. Fuzzy logic speed controller and proportional-integral (PI) current controllers were utilized [23]. MRAC controller accurately provided the actual speed and the rotor position of the PMSM [24]. Design of PI controllers were employed utilizing zero-pole elimination approach for both speed controller and current controllers [25]. Combination of predictive current control and FOC brought improved properties for PMSM drive [26]. For lowering harmonic current, 24-sector vector space decomposition method was implemented [27]. Artificial neural network was inserted into FOC to provide fast response [28]. Adaptive control was applied to control robot-assisted force in FOC drive system [29]. A fractional PI speed controller was used for speed tracking and load rejection performance [30]. Predictive control was assessed in PMSM drive using FOC [31]. Super-twisting sliding mode strategy gave small-overshoot response [32]. Adaptive neuro fuzzy inference mechanism enhanced dynamic performance [33]. Selection of 4-manifolds of stator current provided fast response [34]. In order to obtain linear model of PMSM, an input-output feedback linearization method was applied [35]. The methods listed above are difficult to be implemented on EV. In the paper, a desired transient response-based approach is applied to PI speed controller for simplified model of PMSM drive using SVPWM-FOC.

2. FIELD ORIENTED CONTROL STRUCTURE FOR PMSM DRIVE

Field-oriented-control structure for PMSM drive is shown in Figure 1. The PMSM is mathematically modeled in $\alpha\beta$ stationary reference frame according to (1)-(5).

$$u_{s\alpha} = R_s i_{s\alpha} + \frac{d\psi_{s\alpha}}{dt} \tag{1}$$

$$u_{s\beta} = R_s i_{s\beta} + \frac{d\psi_{s\beta}}{dt} \tag{2}$$

$$\psi_{s\alpha} = L_s i_{s\alpha} + \Phi_F \cos\theta_r \tag{3}$$

$$\psi_{s\beta} = L_s i_{s\beta} + \Phi_F \sin\theta_r \tag{4}$$

$$T_e = 1.5 n_p (i_{s\beta}\psi_{s\alpha} - i_{s\alpha}\psi_{s\beta}) \tag{5}$$

Where: $u_{s\alpha}$, $u_{s\beta}$, $i_{s\alpha}$, $i_{s\beta}$, $\psi_{s\alpha}$, $\psi_{s\beta}$ are elements in $\alpha\beta$ frame of stator voltage, current, flux vectors; R_s, L_s - stator resistance, inductance; Φ_F - PM magnetic flux; θ_r - position of rotor; n_p - number of pole pairs. In case of drive for EV, relationship of motor torque T_e, load torque T_L, and mechanical speed ω_m is expressed by (6):

$$T_e = T_L + J_m \frac{d\omega_m}{dt} + B_m \omega_m \tag{6}$$

where J_m - moment of inertia; B_m - rotational damping constant. Parameters of PMSM are listed in Table 1. Clarke Transformation block estimates $\alpha\beta$ stator current elements according to (7)-(8).

$$\hat{\imath}_{s\alpha} = i_{sa} \tag{7}$$

$$\hat{\imath}_{s\beta} = \frac{(i_{sa} + 2 i_{sb})}{\sqrt{3}} \tag{8}$$

Park transformation block uses (9)-(10) to obtain flux I_d and torque I_q components of stator current:

$$I_d = \hat{\imath}_{s\alpha} \cos\theta_r + \hat{\imath}_{s\beta} \sin\theta_r \tag{9}$$

$$I_q = -\hat{\imath}_{s\alpha} \sin\theta_r + \hat{\imath}_{s\beta} \cos\theta_r \tag{10}$$

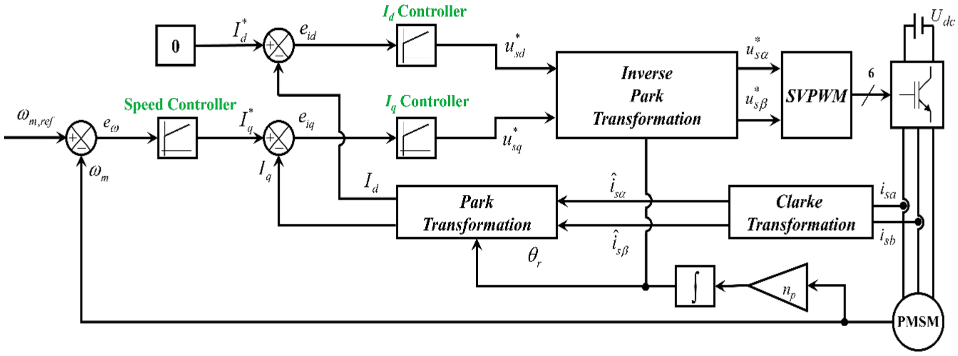

Figure 1. FOC structure for PMSM drive.

Three proportional-integral (PI) controllers including flux-component and torque-component currents, speed one's output reference values of flux u_{sd} and torque u_{sq} components of stator voltages, I_q respectively in Figure 2 according to (11)-(13).

$$u_{sd}^*(s) = K_{pd}\left(1 + \frac{1}{T_{id}s}\right)e_{id}(s) \tag{11}$$

$$u_{sq}^*(s) = K_{pq}\left(1 + \frac{1}{T_{iq}s}\right)e_{iq}(s) \tag{12}$$

$$I_q^*(s) = K_{p\omega}\left(1 + \frac{1}{T_{i\omega}s}\right)e_{\omega}(s) \tag{13}$$

Where K_{pd}, K_{pq}, $K_{p\omega}$; T_{id}, T_{iq}, $T_{i\omega}$ are respectively proportional gains; integral constant times of PI controllers. In order to maximize the torque component current I_q, desired flux component current is chosen to be zero. Inverse Park Transformation block employs position of rotor, desired flux-component and torque-component voltages to obtain desired $\alpha\beta$ stator voltage elements. The SVPWM block uses the desired voltage to obtain switching diagram for IGBTs of three-phase VSI in a switching period.

In order to design PI controllers, block diagrams of control systems are simplified as shown in Figure 2. In case of I_d current control system as shown in Figure 2(a), its transfer function is expressed by (14):

$$G_{Id}(s) = \frac{I_d(s)}{I_d^*(s)} = \frac{K_{pd}[\frac{(T_{id}s+1)}{\{T_{id}s(L_ds+R_s)\}}]}{1+K_{pd}[\frac{(T_{id}s+1)}{\{T_{id}s(L_ds+R_s)\}}]} \tag{14}$$

The parameters of I_d current controller are chosen as (15) thanks to zero-pole elimination approach [23]:

$$T_{id} = \frac{L_d}{R_s} \tag{15}$$

$$K_{pd} = 2\pi f_d L_d \tag{16}$$

$$f_d = k_f f_s \tag{17}$$

where f_s is switching frequency of the inverter, k_f is selected in range [0.05; 0.2] to minimize THD. The transfer function is written as (18).

$$G_{Id}(s) = \left[(2\pi k_f f_s)^{-1}s + 1\right]^{-1} \tag{18}$$

Similarly, let K_{pq}, T_{iq}, f_q following (19)-(21) and utilize simple conversions to obtain transfer function of I_q current control system in Figure 2(b) according to (22).

$$T_{iq} = \frac{L_q}{R_s} \tag{19}$$

$$K_{pq} = 2\pi f_q L_q \tag{20}$$

$$f_q = k_f f_s \tag{21}$$

$$G_{Iq}(s) = \left[(2\pi k_f f_s)^{-1}s + 1\right]^{-1} \tag{22}$$

In order to obtain transfer function of motor speed control system in Figure 2(c), parameters K_{pd}, T_{id}, L_d, R_s in I_d current control system are respectively substituted by $K_{p\omega}/k_t$, $T_{i\omega}$, J_m, B_m, as follows:

$$T_{i\omega} = \frac{J_m}{B_m} \tag{23}$$

$$K_{p\omega} = 2\pi f_\omega J_m k_t \tag{24}$$

$$G_{\omega m}(s) = [(2\pi f_\omega)^{-1}s + 1]^{-1} \tag{25}$$

$$k_t = \frac{K_T}{\sqrt{2}} = \frac{T_N}{(\sqrt{2}I_N)} \tag{26}$$

where K_T is torque constant. Because response times of mechanical systems are longer than electrical systems, f_ω is chosen slower than f_d and f_q:

$$f_\omega = 0.01 f_s \tag{27}$$

The transfer function of speed control system is expressed as (28).

$$G_{\omega m}(s) = [(0.02\pi f_s)^{-1}s + 1]^{-1} \tag{28}$$

In practice, rotational damping constant B_m is small shown in Table 1, this leads to long integral constant time $T_{i\omega}$. So, PI speed controller needs to be redesigned. At first, characteristic equation of speed control system is rewritten as (29).

$$s^2 + \left[\frac{(K_{p\omega}k_t + B_m)}{J_m}\right]s + \frac{K_{p\omega}k_t}{(J_m T_{i\omega})} = 0 \tag{29}$$

Utilizing the method in [36], the stability range of $K_{p\omega}$, $T_{i\omega}$ is the one of $K_{p\omega} > 0$, $T_{i\omega} > 0$. For desired overshoot M_p and settling time t_{set} (decaying exponential reaches 1%), parameters of PI speed controller are computed as follows [37]:

$$\zeta = \sqrt{\frac{(\ln M_p^*)^2}{[\pi^2 + (\ln M_p^*)^2]}} \tag{30}$$

$$\omega_n = \frac{-\ln 0.01}{\zeta t_{set}^*} \tag{31}$$

$$K_{p\omega} = \frac{(2\zeta\omega_n J_m - B_m)}{k_t} \tag{32}$$

$$T_{i\omega} = \frac{k_t K_{p\omega}}{(J_m \omega_n^2)} \tag{33}$$

where ζ: damping ratio, ω_n: undamped natural frequency.

Table 1. Parameters of PMSM

Symbol	Quantity	Value	Symbol	Quantity	Value
P_N	Rated power	3.9 kW	n_N	Rate speed	3000 rpm
U_N	Rated voltage	180 V	n_p	Number of pole pairs	3
T_N	Rated torque	12.5 Nm	Φ_F	PM magnetic flux	0.185 Wb
I_N	Rated current	14.9 A	R_s	Stator resistance	0.3 Ω
J_m	Motor inertia	0.0755 kgm^2	L_q, L_d	q-axis, d-axis inductances	8.5 mH
B_m	Rotational damping constant	0.001 Nm.s			

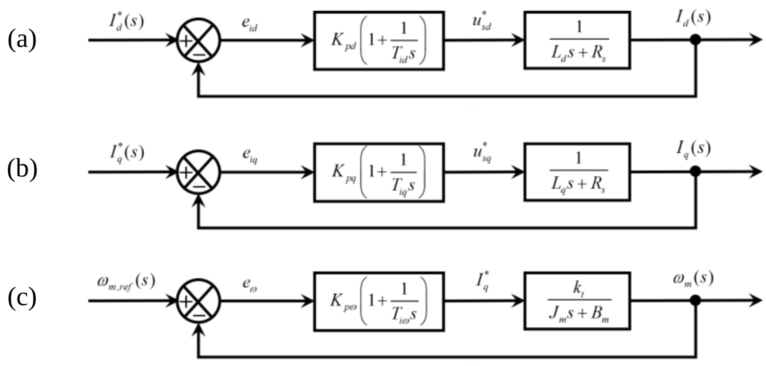

Figure 2. Block diagram of control systems: (a) I_d current, (b) I_q current, and (c) motor speed

3. SIMULATION

The MATLAB/Simulink simulations are implemented in cases of $U_{dc} = 440\ V$, $k_f = 0.08$, $\omega_{m,ref} = \{3000\ rpm, 300\ rpm, 30\ rpm\}$, load torque $T_L = 10\ Nm$ activated at 2 second time for two methods: first one is the zero-pole elimination approach with $K_{p\omega} = 56.28$, $T_{i\omega} = 75.5\ s$ (in (23)-(24)) and second one is the desired-transient-response-based approach with desired $M_p = 0.01$ and $t_{set} = 0.1\ s$, $K_{p\omega} = 11.72$, $T_{i\omega} = 29.6\ ms$ (31)-(34). Parameters of I_d and I_q controllers are respectively computed according to (15)-(16) and (19)-(20). Outputs of speed controller, current controllers are limited in ±21.1 A, ±255 V, respectively.

Figures 3-5 show speed and torque-component current responses at reference speed of 3000 rpm, 300 rpm, 30 rpm, respectively. It is easy to see that overshoot in speed and torque-component current responses, and steady-state speed error E_{ss} for 1st method are much larger than those for 2nd method at simulated reference speeds as shown in Figures 3-5. The reason for this is that the integral constant time $T_{i\omega}$ of the 1st method is 2540 times longer than that of the 2nd method. Table 2 shows overshoot, undershoot due to load activation, E_{ss}, and stator current $i_{s\alpha}$ THD with advantages in overshoot, E_{ss}, THD for the 2nd method-proposed method. For undershoot, the 1st approach brings reduction of approximate 60% in comparison to the 2nd method. Figures 5 and 6 show that stator current responses of the 1st method fluctuate more than the 2nd one, especially at times of starting and change of load torque. This leads to THD of the 1st design approach significantly higher than the 2nd one.

Table 2. Performances of two PI speed controller design methods.

$\omega_{m,ref}$	Overshoot [rpm]		Undershoot [rpm]		Steady-state error [rpm]		Current THD [%]	
	1st method	2nd method	1st method	2nd method	1st method	2nd method	1st method	2nd method
3000	0.063	0.013	1.025	1.041	0.220	0.0005	1.07	1.07
300	0.544	0.034	0.398	0.955	0.211	0.0001	0.45	0.39
30	0.598	0.035	0.382	0.956	0.211	0.0002	1.33	0.23

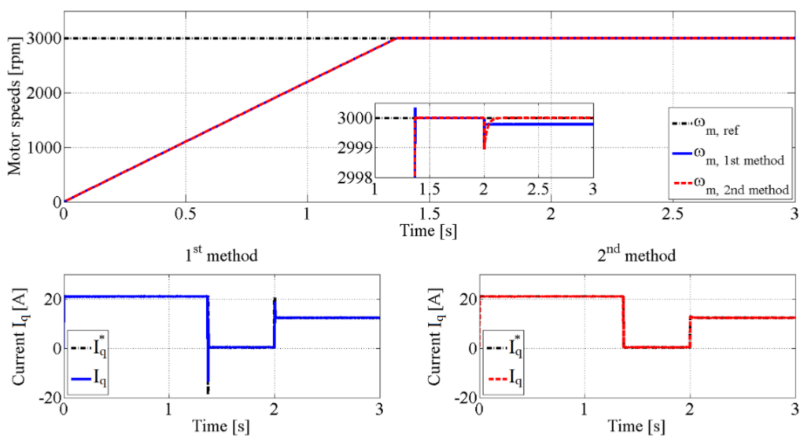

Figure 3. Motor speeds (upper) and torque-component currents at $\omega_{m,ref}$ = 3000 rpm

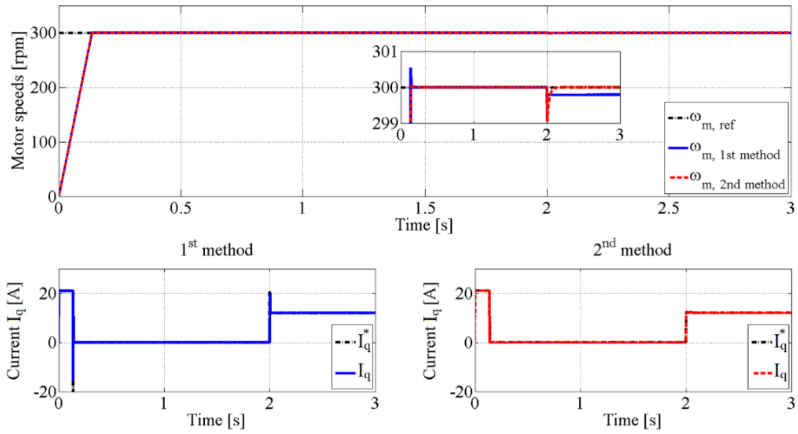

Figure 4. Motor speeds (upper) and torque-component currents at $\omega_{m,ref}$ = 300 rpm

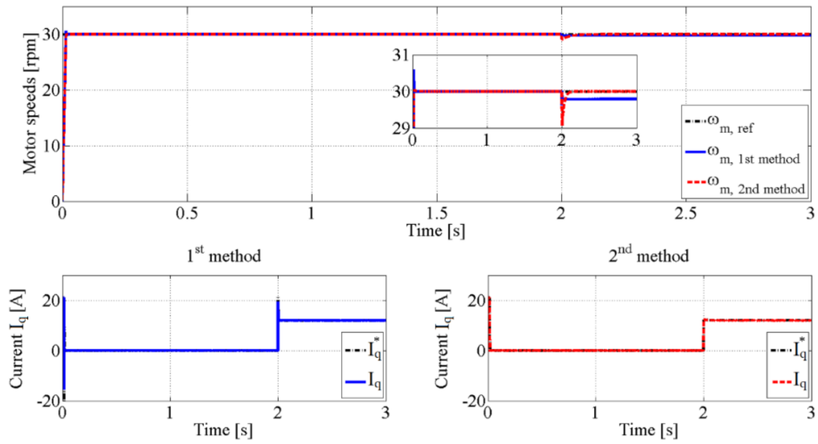

Figure 5. Motor speeds (upper) and torque-component currents at $\omega_{m,ref}$ =30 rpm

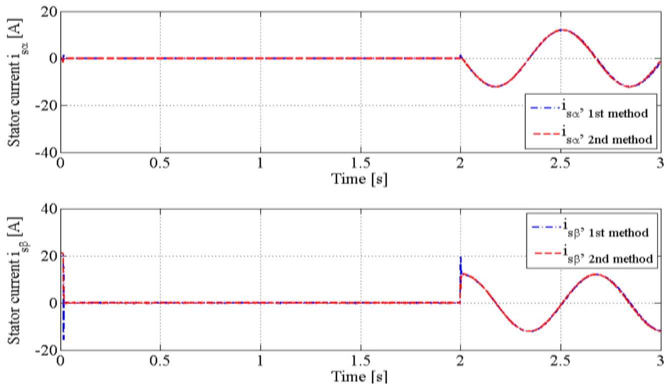

Figure 6. Stator currents at $\omega_{m,ref}$ =30 rpm

4. CONCLUSION

The paper presents the application of zero-pole elimination and desired-transient-response-based methods in design of PI speed controller for FOC PMSM drive of a simplified model of an EV. The performances of drive system with two approaches were verified in simulation environment. The proposed desired-transient-response-based method provided higher performance with lower overshoot, smaller steady-state speed error, and reduction in stator current THD in comparison to zero-pole elimination method. However, robustness to load change of zero-pole elimination one is higher than the proposed one. Other advanced controllers can be utilized to achieve better performance.

ACKNOWLEDGEMENTS

Author specially thanks Professor Min-Fu Hsieh, National Cheng Kung University, Tainan, Taiwan for his enthusiastic guidance in completing the graduation project of Mr. Le.

REFERENCES

[1] B. K. Bose, "Global energy scenario and impact of power electronics in 21st century," *IEEE Transactions on Industrial Electronics*, vol. 60, no. 7, pp. 2638–2651, 2013, doi: 10.1109/TIE.2012.2203771.

[2] A. A. E. B. A. El Halim, E. H. E. Bayoumi, W. El-Khattam, and A. M. Ibrahim, "Electric vehicles: a review of their components and technologies," *International Journal of Power Electronics and Drive Systems*, vol. 13, no. 4, pp. 2041–2061, 2022, doi: 10.11591/ijpeds.v13.i4.pp2041-2061.

[3] S. A. Saleh and A. Rubaai, "Extending the Frame-angle-based direct torque control of PMSM drives to low-speed operation," *IEEE Transactions on Industry Applications*, vol. 55, no. 3, pp. 3138–3150, 2019, doi: 10.1109/TIA.2018.2890060.

[4] S. S. Hakami and K. B. Lee, "Modified direct torque control for fast dynamics PMSM drives fed by three-level NPC inverter," *ICEMS 2021 - 2021 24th International Conference on Electrical Machines and Systems*, pp. 636–640, 2021, doi: 10.23919/ICEMS52562.2021.9634461.

[5] A. Nasr, C. Gu, X. Wang, G. Buticchi, S. Bozhko, and C. Gerada, "Torque-performance improvement for direct torque-controlled PMSM drives based on duty-ratio regulation," *IEEE Transactions on Power Electronics*, vol. 37, no. 1, pp. 749–760, Jan. 2022, doi: 10.1109/TPEL.2021.3093344.

[6] L. Yu, C. Wang, H. Shi, R. Xin, and L. Wang, "Simulation of PMSM field-oriented control based on SVPWM," in *2017 29th Chinese Control And Decision Conference (CCDC)*, May 2017, pp. 7407–7411, doi: 10.1109/CCDC.2017.7978524.

[7] Suryakant, M. Sreejeth, and M. Singh, "Performance analysis of PMSM drive using hysteresis current controller and PWM current controller," *2018 IEEE International Students' Conference on Electrical, Electronics and Computer Science, SCEECS 2018*, 2018, doi: 10.1109/SCEECS.2018.8546862.

[8] M. Slunjski, O. Stiscia, M. Jones, and E. Levi, "General torque enhancement approach for a nine-phase surface PMSM with built-in fault tolerance," *IEEE Transactions on Industrial Electronics*, vol. 68, no. 8, pp. 6412–6423, 2021, doi: 10.1109/TIE.2020.3007053.

[9] H. Yao, Y. Yan, T. Shi, G. Zhang, Z. Wang, and C. Xia, "A novel SVPWM scheme for field-oriented vector-controlled PMSM drive system fed by cascaded h-bridge inverter," *IEEE Transactions on Power Electronics*, vol. 36, no. 8, pp. 8988–9000, 2021, doi: 10.1109/TPEL.2021.3054642.

[10] M. Furmanik, M. Vidlak, and P. Rafajdus, "Current harmonics control in six-phase PMSM," *14th International Conference ELEKTRO, ELEKTRO 2022 - Proceedings*, 2022, doi: 10.1109/ELEKTRO53996.2022.9803632.

[11] Z. Novak and M. Novak, "Adaptive PLL-based sensorless control for improved dynamics of high-speed PMSM," *IEEE Transactions on Power Electronics*, vol. 37, no. 9, pp. 10154–10165, 2022, doi: 10.1109/TPEL.2022.3169708.

[12] H. H. Vo, P. Brandstetter, T. C. Tran, and C. S. T. Dong, "An implementation of rotor speed observer for sensorless induction motor drive in case of machine parameter uncertainty," *Advances in Electrical and Electronic Engineering*, vol. 16, no. 4, pp. 426–434, 2018, doi: 10.15598/aeee.v16i4.2973.

[13] G. N. Chethan and G. Kodeeswara Kumaran, "Performance analysis of PMSM drive with spacevector PWM and sinusoidal PWM fed VSI," *1st International Conference on Power Electronics Applications and Technology in Present Energy Scenario, PETPES 2019 - Proceedings*, 2019, doi: 10.1109/PETPES47060.2019.9003961.

[14] T. Suzuki, Y. Hayashi, H. Kabune, and N. Ito, "Pulsewidth modulation control algorithm for a six-phase PMSM: reducing the current in the inverter capacitor and current sensing with resistors," *IEEE Transactions on Industrial Electronics*, vol. 66, no. 6, pp. 4240–4249, 2019, doi: 10.1109/TIE.2018.2863192.

[15] H. Mahmoudi, M. Aleenejad, and R. Ahmadi, "Torque ripple minimization for a permanent magnet synchronous motor using a modified quasi-z-source inverter," *IEEE Transactions on Power Electronics*, vol. 34, no. 4, pp. 3819–3830, 2019, doi: 10.1109/TPEL.2018.2852753.

[16] M. Khalid, A. Mohan, and A. C. Binojkumar, "Performance analysis of vector controlled PMSM drive modulated with sinusoidal PWM and space vector PWM," *2020 IEEE International Power and Renewable Energy Conference, IPRECON 2020*, 2020, doi: 10.1109/IPRECON49514.2020.9315210.

[17] S. Jayaprakasan, A. Ashok, and R. Ramchand, "Current error space vector based hysteresis controller for VSI fed PMSM drive," *IEEE Transactions on Power Electronics*, vol. 35, no. 10, pp. 10690–10699, 2020, doi: 10.1109/TPEL.2020.2977581.

[18] H. H. Vo, D. Q. Nguyen, Q. T. Nguyen, C. S. T. Dong, T. C. Tran, and P. Brandstetter, "Pulse-width modulation direct torque control induction motor drive with Kalman filter," *Telkomnika (Telecommunication Computing Electronics and Control)*, vol. 19, no. 1, pp. 277–284, 2021, doi: 10.12928/TELKOMNIKA.V19I1.16247.

[19] V. Repecho, A. Sierra-Gonzalez, E. Ibarra, D. Biel, and A. Arias, "Enhanced DC-link voltage utilization for sliding-mode-controlled PMSM drives," *IEEE Journal of Emerging and Selected Topics in Power Electronics*, vol. 9, no. 3, pp. 2850–2857, 2021, doi: 10.1109/JESTPE.2020.3009522.

[20] S. K. Singh and A. Tripathi, "Synchronized sine-triangle PWM based control of high-speed PMSM drive with reduced switching losses and enhanced performance," *2022 IEEE Delhi Section Conference, DELCON 2022*, 2022, doi: 10.1109/DELCON54057.2022.9753230.

[21] T. Hara *et al.*, "Synchronous PWM control with carrier wave phase shifts for permanent magnet synchronous motor," *IEEE Transactions on Industry Applications*, vol. 58, no. 5, pp. 5650–5658, 2022, doi: 10.1109/TIA.2022.3187679.

[22] C. Dong, P. Brandstetter, H. H. Vo, T. C. Tran, and D. H. Vo, "Adaptive sliding mode controller for induction motor," *Lecture Notes in Electrical Engineering*, vol. 415 LNEE, pp. 543–553, 2017, doi: 10.1007/978-3-319-50904-4_58.

[23] Y. M. Alsayed, A. Maamoun, and A. Shaltout, "High performance control of PMSM drive system implementation based on DSP real-time controller," *Proceedings of 2019 International Conference on Innovative Trends in Computer Engineering, ITCE 2019*, pp. 225–230, 2019, doi: 10.1109/ITCE.2019.8646462.

[24] S. Suryakant, M. Sreejeth, and M. Singh, "Sensorless control of PMSM Drive with BEMF based MRAC Algorithm," *2019 International Symposium on Advanced Electrical and Communication Technologies, ISAECT 2019*, 2019, doi: 10.1109/ISAECT47714.2019.9069705.

[25] M. F. Hsieh, N. C. Chen, and T. D. Ton, "System response of permanent magnet synchronous motor drive based on SiC power transistor," *2019 IEEE 4th International Future Energy Electronics Conference, IFEEC 2019*, 2019, doi: 10.1109/IFEEC47410.2019.9015197.

[26] L. Ashok Kumar and V. Indragandhi, "PMSM drive using predictive current control technique for HVAC applications," *Proceedings of International Conference on Artificial Intelligence, Smart Grid and Smart City Applications*, pp. 31–41, 2020, doi: 10.1007/978-3-030-24051-6_4.

[27] M. Hasoun, A. El Afia, M. Khafallah, and K. Benkirane, “Field oriented control based on a 24-sector vector space decomposition for dual three-phase pmsm applied on electric ship propulsion,” *International Journal of Power Electronics and Drive Systems*, vol. 11, no. 3, pp. 1175–1187, 2020, doi: 10.11591/ijpeds.v11.i3.pp1175-1187.

[28] S. S. Rauth and B. Samanta, “Comparative analysis of IM/BLDC/PMSM drives for electric vehicle traction applications using ANN-based FOC,” *2020 IEEE 17th India Council International Conference, INDICON 2020*, 2020, doi: 10.1109/INDICON49873.2020.9342237.

[29] K. Huang, P. Liu, H. Peng, D. Du, and X. Xia, “Robot auxiliary suspension and control feedback system,” *Proceedings - 2020 Chinese Automation Congress, CAC 2020*, pp. 611–617, 2020, doi: 10.1109/CAC51589.2020.9327871.

[30] D. M. Kumar, M. Cirrincione, H. K. Mudaliar, M. Di Benedetto, A. Lidozzi, and A. Fagiolini, “Development of a fractional PI controller in an FPGA environment for a robust high-performance PMSM electrical drive,” *Proceedings of the Energy Conversion Congress and Exposition - Asia, ECCE Asia 2021*, pp. 2427–2431, 2021, doi: 10.1109/ECCE-Asia49820.2021.9479450.

[31] N. Pardo, H. Young, and N. Aros-Onate, “Evaluation of predictive torque control of a PMSM under model parameter mismatch,” *2021 IEEE CHILEAN Conference on Electrical, Electronics Engineering, Information and Communication Technologies, CHILECON 2021*, 2021, doi: 10.1109/CHILECON54041.2021.9702917.

[32] N. T. Dat, C. Van Kien, and H. P. H. Anh, “Hybrid super-twisting sliding mode and FOC scheme for advanced PMSM driving control,” *Lecture Notes in Mechanical Engineering*, pp. 776–780, 2022, doi: 10.1007/978-3-030-99666-6_112.

[33] S. Ranjan, M. Sreejeth, and M. Singh, “Analysis of the performance of an HCC based PMSM drive using adaptive neuro fuzzy inference,” *2022 2nd International Conference on Intelligent Technologies, CONIT 2022*, 2022, doi: 10.1109/CONIT55038.2022.9848167.

[34] M. K. B. Boumegouas and K. Kouzi, “A new synergetic scheme control of electric vehicle propelled by six-phase permanent magnet synchronous motor,” *Advances in Electrical and Electronic Engineering*, vol. 20, no. 1, pp. 1–14, 2022, doi: 10.15598/aeee.v20i1.4221.

[35] B. Abdellah, H. Abdeldjebar, and K. Medjdoub, “An application for nonlinear control by input-output linearization technique for pm synchronous motor drive for electric vehicles,” *International Journal of Power Electronics and Drive Systems*, vol. 13, no. 4, pp. 1984–1992, 2022, doi: 10.11591/ijpeds.v13.i4.pp1984-1992.

[36] H. H. Vo, P. Brandstetter, C. S. T. Dong, T. Q. Thieu, and D. H. Vo, “An implementation on MATLAB software for stability analysis of proportional controllers in linear time invariant control systems,” *Advances in Intelligent Systems and Computing*, vol. 444, pp. 671–680, 2016, doi: 10.1007/978-3-319-31232-3_63.

[37] G. F. Franklin, D. Powell, and A. F. Emami-Naeini, “Dynamic Response,” in *Feedback Control of Dynamic Systems*, H. S. Sanjay, Ed., 7th ed. London, United Kingdom: Pearson, 2015, pp. 151–156.

BIOGRAPHIES OF AUTHORS

Chau Si Thien Dong obtained the Ph.D. degree from Faculty of Electrical Engineering and Computer Science (FEECS), Technical University of Ostrava (VSB-TUO), Czech Republic in 2017. She is now dean of FEEE, TDTU, Vietnam. She has published 15 conference papers and 8 journal papers. Her research interests focus on modern electrical drives, nonlinear control, adaptive control, robust control, and neural network. She can be contacted at email: dongsithienchau@tdtu.edu.vn.

Hoang Huy Le has been obtaining the B.Eng. degree in automation and control engineering from FEEE, TDTU, Vietnam. His research interests are modern methods of electrical drives for Vehicles. He can be contacted at email: 41703076@student.tdtu.edu.vn or lhhoang99@gmail.com.

Hau Huu Vo was born in Binh Thuan, Vietnam. He received the B.Eng. degree in mechatronics engineering, and the M.Sc. degree in automatic control from University of Technology, Vietnam National University – HCMC, in 2006 and 2009, respectively. He has been working as a Lecturer at FEEE, TDTU, since 2010. He holds a Ph.D. degree from VSB-TUO, Czech Republic in 2017. He has published 10 journal papers. His research interests are modern electrical drives. He can be contacted at email: vohuuhau@tdtu.edu.vn.